G12 Track Normalization Procedure

Michael C. Kunkel

November 14, 2018

1 Normalization

1.1 Normalization History

In the g11 experiment there is an 18% discrepancy between the differential cross-sections of $\gamma p \to p\omega$ measured channels $\gamma p \to p\pi^+\pi^-(\pi^0)$ and $\gamma p \to p\pi^+(\pi^-\pi^0)$. One method of correction for this effect was to apply a global scale factor to the two track topology. The scale factor was on the order of 18%. The cause of the inefficiency was unknown but is believed to be due to the high current of the electron beam in conjunction with requiring 3 charged tracks from a 2-prong trigger.

1.2 g12 Normalization Procedure

In this analysis, a normalization constant on the order of 18% was also needed. The cause of this effect is unknown, but it is also believed to be related to using 3 charged tracks from 2-prong triggers at high current. GPP is responsible for smearing and dropping inefficient parts of the detector but not trigger efficiency. Therefore the normalization could be simulated if it was a trigger effect or another happenstance related to requiring 3 charged tracks in the analysis. To investigate this effect the following 3 topologies;

$$\gamma p \to p\pi^+(\pi^-)$$
$$\gamma p \to p\pi^-(\pi^+)$$
$$\gamma p \to \pi^+\pi^-(p) \tag{1}$$

were skimmed from data and simulated using the prescription chain in the approved G12 analysis procedures [1]. In order to eliminate any statistical effects, $\frac{1}{4}$ of the entire g12 data set was used and over 1 billion events were generated for simulation. Table 1 lists the number of events analyzed for each of the topologies listed in Eq. 1. The data had two orders of magnitude

higher statistics than the simulation, this was done to ensure enough events

Topology	Data Reconstructed	Monte-Carlo Generated/Reconstructed
$\gamma p \to p\pi^+(\pi^-)$	$5.09 \cdot 10^{10}$	$1.2 \cdot 10^9$ / $2.16 \cdot 10^8$
$\gamma p \to p\pi^-(\pi^+)$	$5.43 \cdot 10^{10}$	$1.2 \cdot 10^9$ / $2.17 \cdot 10^8$
$\gamma p \to \pi^+\pi^-(p)$	$5.34 \cdot 10^{10}$	$1.2 \cdot 10^9$ / $1.08 \cdot 10^8$

Table 1: Number of Events Used in Efficiency Study

to analyze in the high momentum spectrum. The simulation generated the listed reactions in phase space using PLUTO++ as the phase space generator . The data and simulation were analyzed in the same manner.

The data was skimmed under the conditions of Eq. 1. If the missing particle (particle in parenthesis) was detected, then this information was also recorded. After the data was skimmed, kinematic fits (1-C) were performed to the missing particles. Nominal geometric fiducial cuts were employed for all detected particles along with a pull probability for each topology > 1 %, see Fig. 1.
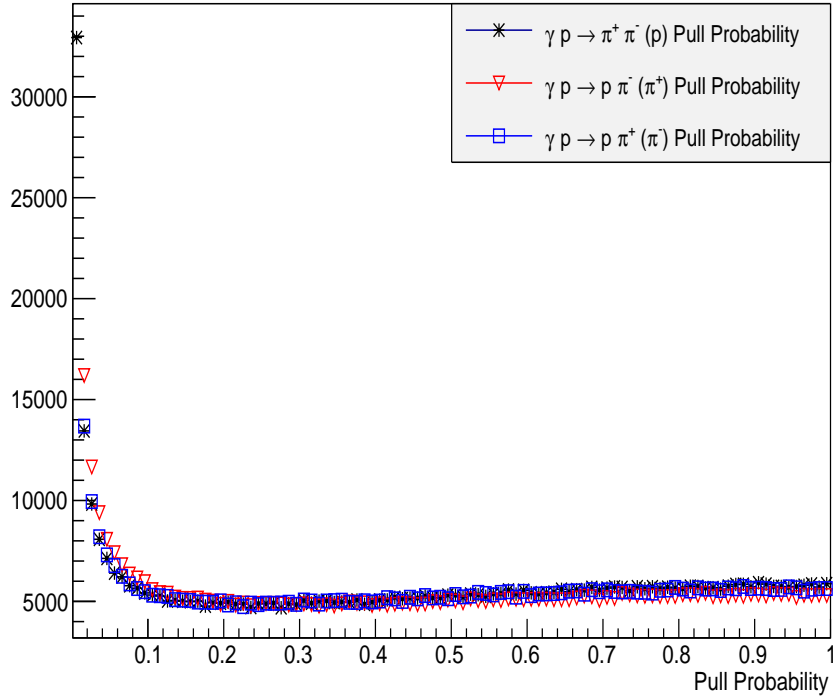
Pull Probabilities for Normalization Study

Figure 1: Number of events vs. the 1-C pull probability distribution for the reactions used in the normalization study for data.
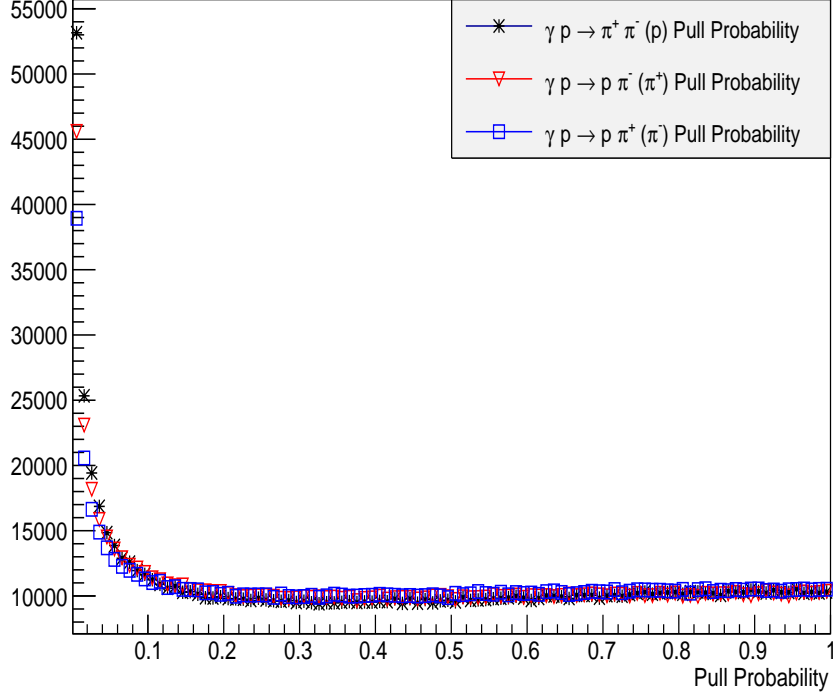
Figure 2: Number of events vs. the 1-C pull probability distribution for the reactions used in the normalization study for MC.

The z-vertex of the two needed particles was determined by the method of distance of closest approach of the two vectors. The data was then binned for the fitted missing particle according to the z-vertex position, momentum, $\theta \sin \phi$, and $\theta \cos \phi$. The z-vertex and momentum binning used can be seen in Table 2. If the particle to be fit was detected by CLAS, the information was also binned according z-vertex, momentum, $\theta \sin \phi$, and $\theta \cos \phi$. However to ensure that the detected particle and the fitted missing particle were the same, the detected particle must have been in the same momentum bin as the fitted missing particle.

The $\theta \sin \phi$ and $\theta \cos \phi$ binning was chosen to interpret the geometric x and y space the particle travels, independent of momentum and x and y vertex. These $\theta \sin \phi$ and $\theta \cos \phi$ quantities are plotted as x and y variable of a histogram. To better illustrate this interpretation consider a spherical

z bins [cm] (5 cm increments)	Momentum bins [GeV]
	0 - 0.5
	0.5 - 0.75
	0.75 - 1
-70 cm $<\ z\ < -110$ cm	1 - 1.5
	1.5 - 2
	2 - 2.5
	2.5 - 3
	3 - 5

Table 2: Binning Used in the Efficiency Study.

coordinate system where;

$$r = \sqrt{x^2 + y^2 + z^2} \tag{2}$$
$$x = r \sin\theta \cos\phi \tag{3}$$
$$y = r \sin\theta \sin\phi \tag{4}$$

therefore,

$$\theta \sin\phi = \left(\frac{\theta}{r \sin\theta}\right) y \tag{5}$$

$$\theta \cos\phi = \left(\frac{\theta}{r \sin\theta}\right) x\ . \tag{6}$$

It can be seen that plotting Eq 6 versus Eq 5 projects $x - y$ space.

For each type of missing particle, we plotted the number of events versus $\theta \sin\phi$ and $\theta \cos\phi$. We then plotted the number of events where the "missing" particle was detected. The ratio of the number of detected "missing" particle to the total number of "missing" particles is the detection efficiency for that bin in z-vertex, p, $\theta \sin\phi$ and $\theta \cos\phi$ (see Figs 3, 6 and 9). This process was repeated for simulated data (see Figs 4, 7 and 10). The ratio of the simulated efficiency to the measured efficiency for each particle was used to correct the data (see Figs 5, 8 and 11). This procedure revealed any differences between the real and simulated detector responses.

1.3   g12 Normalization Results

It was noticed that the simulation was over-efficient as compared to the data and the ratio of the efficiency of reconstruction should suffice as a correction to the data. Figures 3, 6, 9 depict the efficiency of data reconstruction for the proton π^+ and π^- respectively. Figures 4, 7, 10 depict the efficiency of the simulation reconstruction for the proton π^+ and π^- respectively. Figures 5, 8, 11 depict the over-efficiency of the simulation to data reconstruction for the proton π^+ and π^- respectively. The total over-efficiency was

calculated as the product of each track's over-efficiency, i.e.,

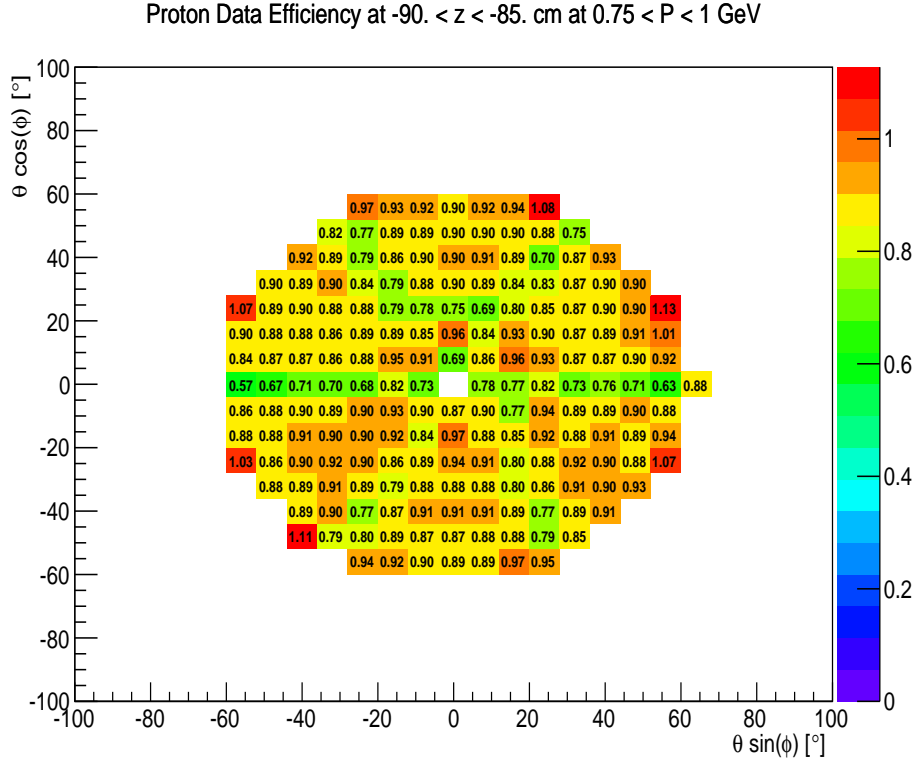$$\epsilon = \epsilon_{proton} \cdot \epsilon_{\pi^+} \cdot \epsilon_{\pi^-}. \tag{7}$$

Figure 3: $\theta\cos\phi$ vs. $\theta\sin\phi$ plot showing the efficiency of detecting the proton with z-vertex $-90 < z < -85$ cm and momentum $0.75 < p < 1$ GeV from a 2 charged track reaction using CLAS detection for g12.
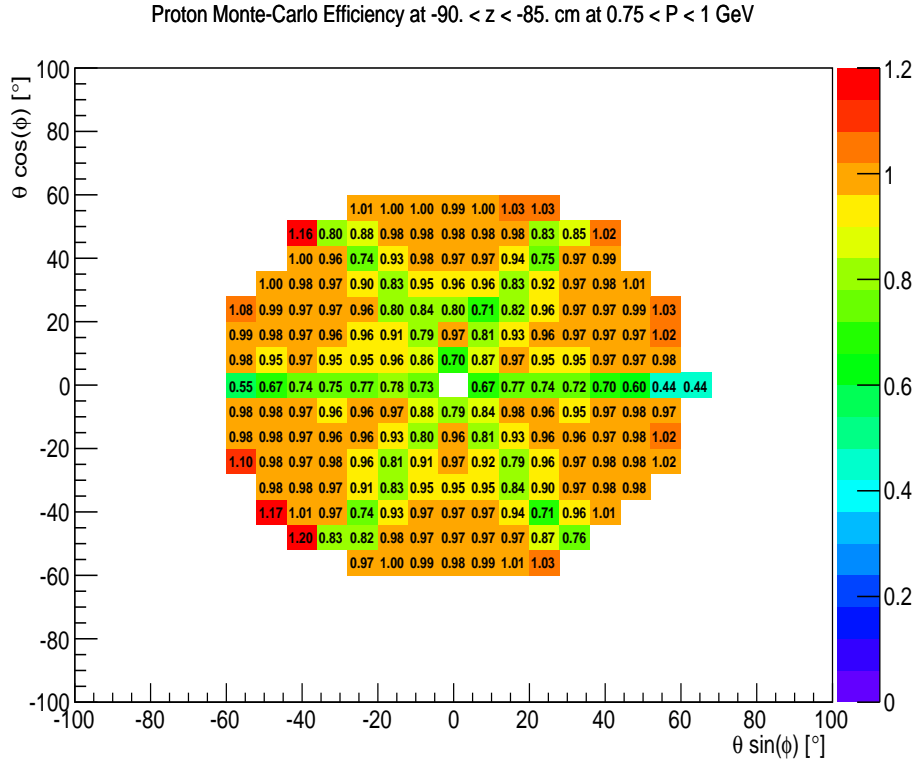
Figure 4: $\theta \cos \phi$ vs. $\theta \sin \phi$ plot showing the efficiency of reconstructing the proton with z-vertex $-90 < z < -85$ cm and momentum $0.75 < p < 1$ GeV from a 2 charged track reaction using CLAS Monte-Carlo for g12.
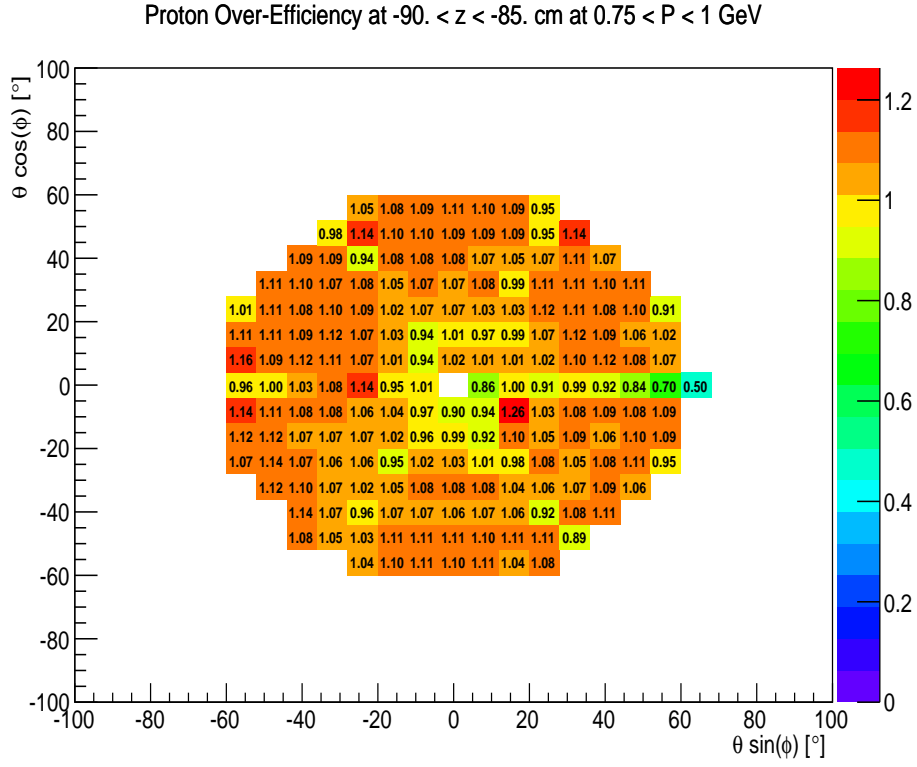
Figure 5: $\theta\cos\phi$ vs. $\theta\sin\phi$ plot showing the over-efficiency of simulating the proton with z-vertex $-90 < z < -85$ cm and momentum $0.75 < p < 1$ GeV from a 2 charged track reaction.
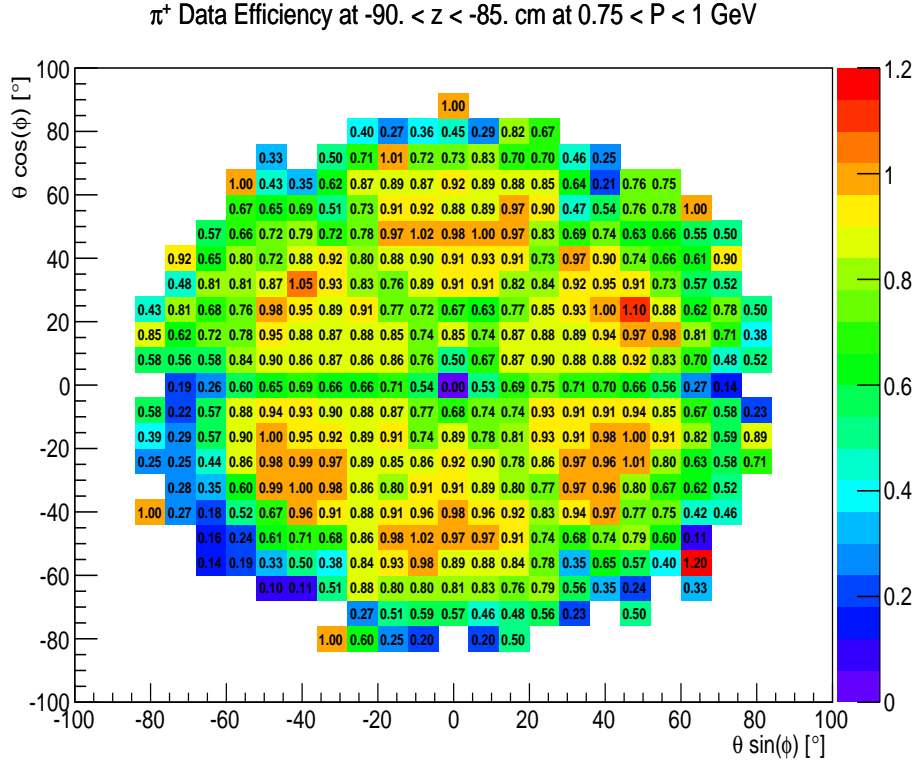
Figure 6: $\theta \cos \phi$ vs. $\theta \sin \phi$ plot showing the efficiency of detecting the π^+ with z-vertex $-90 < z < -85$ cm and momentum $0.75 < p < 1$ GeV from a 2 charged track reaction using CLAS detection for g12.
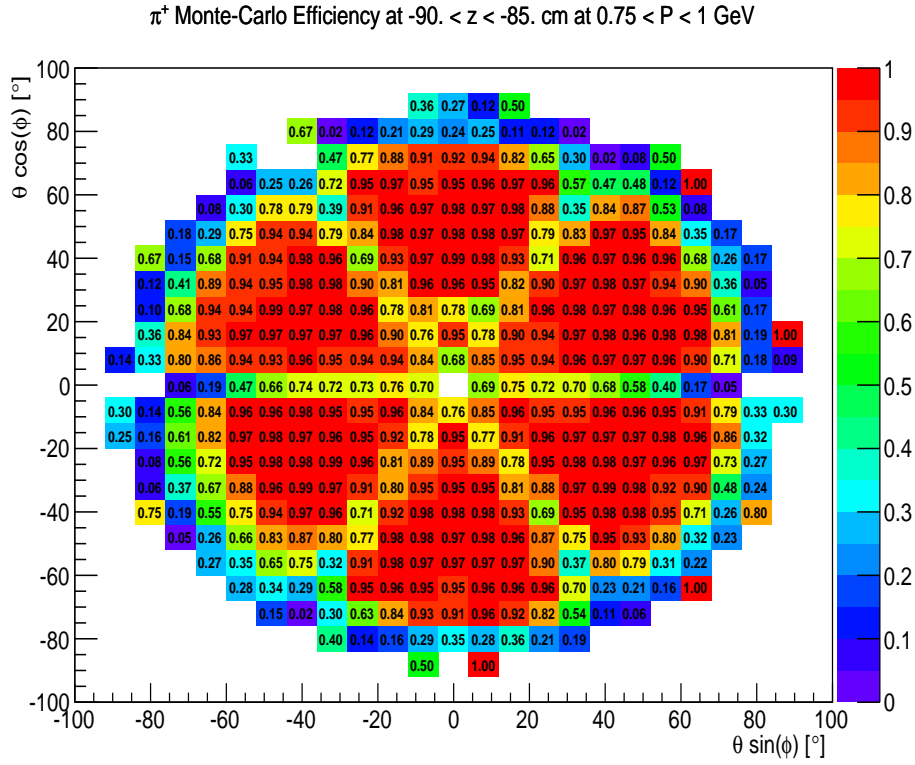
Figure 7: $\theta\cos\phi$ vs. $\theta\sin\phi$ plot showing the efficiency of reconstructing the π^+ with z-vertex $-90 < z < -85$ cm and momentum $0.75 < p < 1$ GeV from a 2 charged track reaction using CLAS Monte-Carlo for g12.
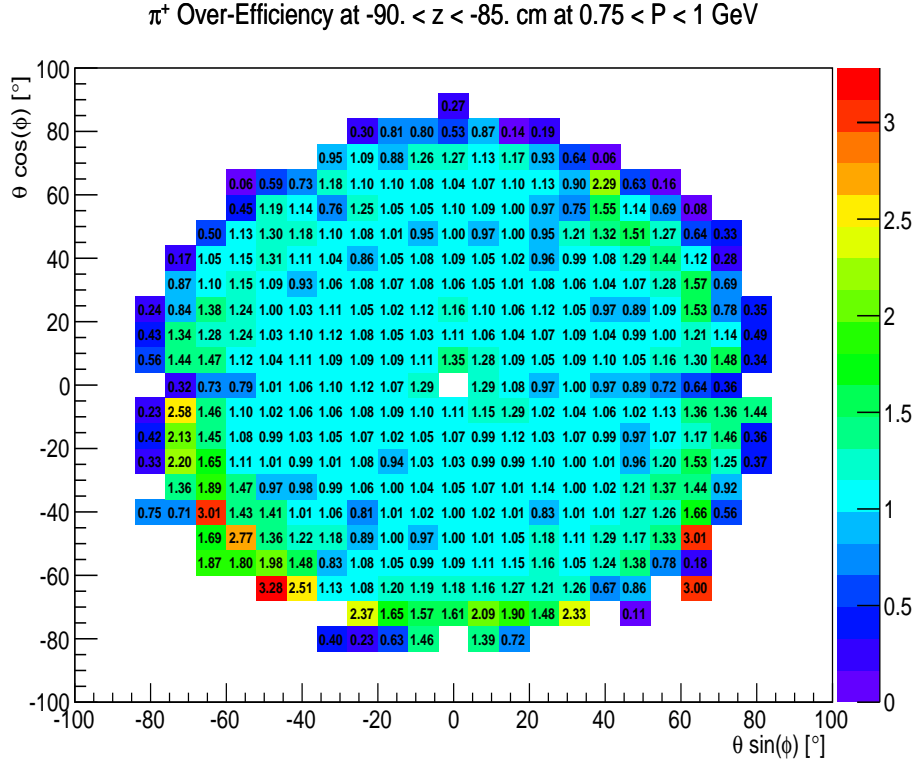
Figure 8: $\theta\cos\phi$ vs. $\theta\sin\phi$ plot showing the over-efficiency of simulating the π^+ with z-vertex $-90 < z < -85$ cm and momentum $0.75 < p < 1$ GeV from a 2 charged track reaction.
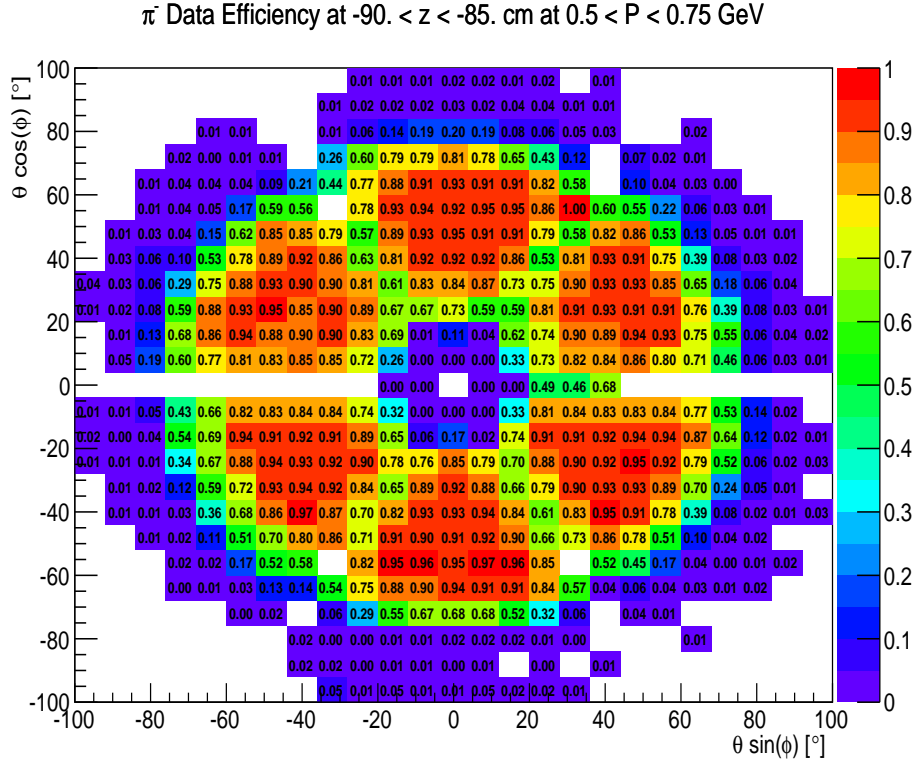
Figure 9: $\theta \cos \phi$ vs. $\theta \sin \phi$ plot showing the efficiency of detecting the π^- with z-vertex $-90 < z < -85$ cm and momentum $0.75 < p < 1$ GeV from a 2 charged track reaction using `CLAS` detection for g12.

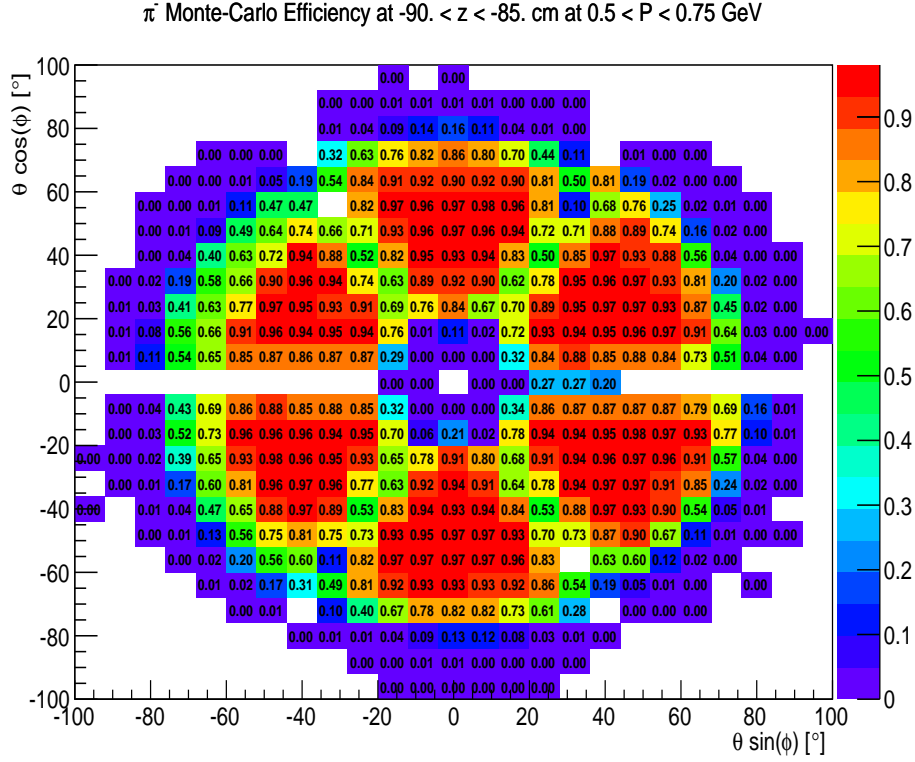π⁻ Monte-Carlo Efficiency at -90. < z < -85. cm at 0.5 < P < 0.75 GeV

Figure 10: $\theta \cos \phi$ vs. $\theta \sin \phi$ plot showing the efficiency of reconstructing the π^- with z-vertex $-90 < z < -85$ cm and momentum $0.75 < p < 1$ GeV from a 2 charged track reaction using CLAS Monte-Carlo for g12.
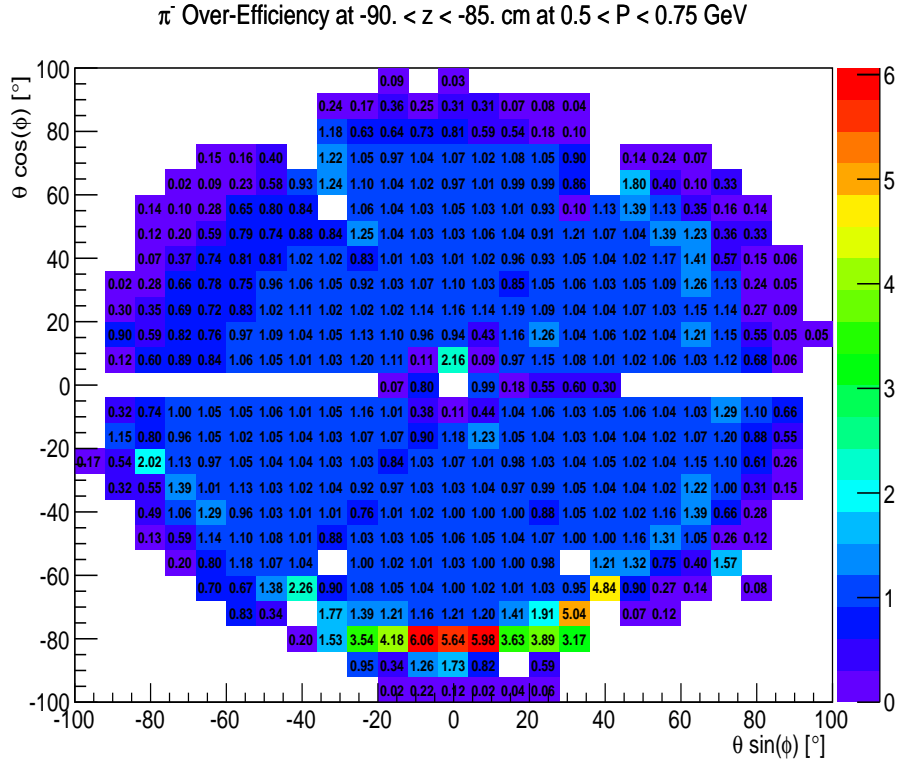
Figure 11: $\theta \cos \phi$ vs. $\theta \sin \phi$ plot showing the over-efficiency of simulating the π^- with z-vertex $-90 < z < -85$ cm and momentum $0.75 < p < 1$ GeV from a 2 charged track reaction.

1.4 Normalization Comparison

To validate the g12 normalization results, the g12 π^0 differential cross-section was calculated using the G11 global normalization factor and then compared to the g12 π^0 differential cross-section using the g12 normalization procedure results. It is shown in Fig. 12 and Fig. 13 that the 2 methods agree with one another except for the very forward regions of $\cos\theta_{C.M.}^{\pi^0}$, where the cross-section using the dynamic normalization is larger than the cross-section measured with the G11 global normalization, however the larger cross-sections at forward $\cos\theta_{C.M.}^{\pi^0}$ agree very well with the past results, see G12 publication [2] for the comparison.

Figure 12: $\frac{d\sigma}{d\Omega}$ vs. $\cos\theta$ plot showing the g12 π^0 differential cross-section when the G11 global normalization is used (blue) and when the g12 dynamic normalization is used (red) for various bins of beam energy inside the lepton trigger acceptance.
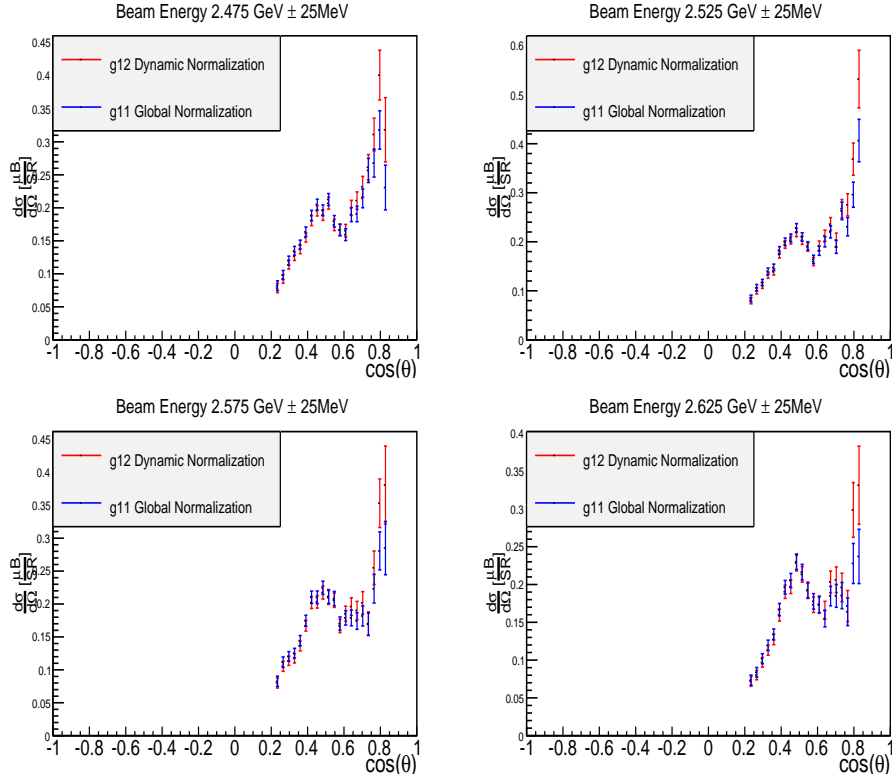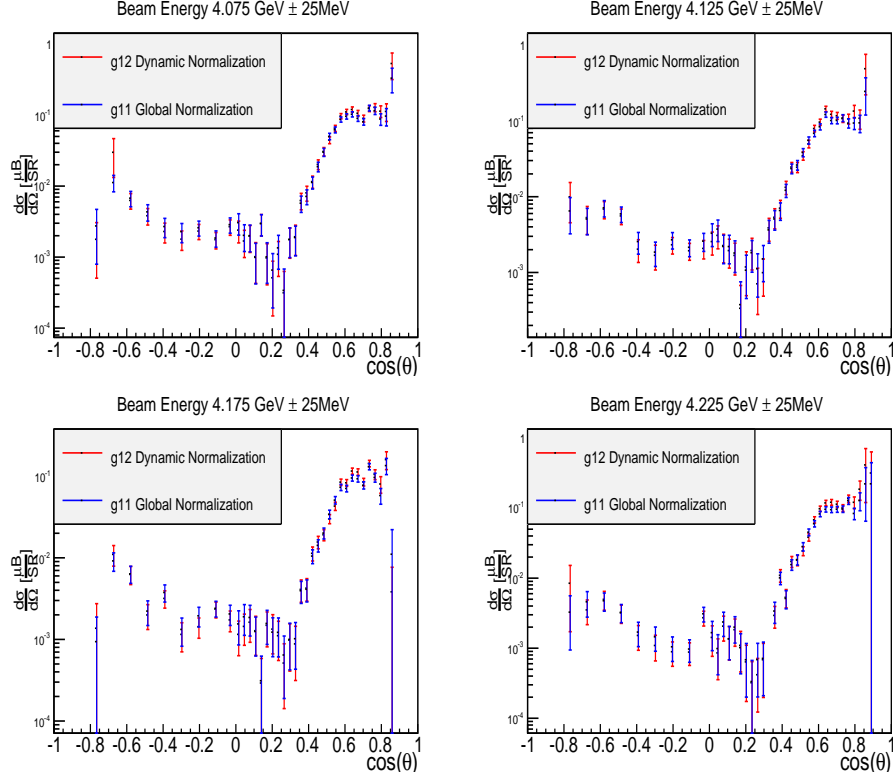
Figure 13: $\frac{d\sigma}{d\Omega}$ vs. $\cos\theta$ plot showing the g12 π^0 differential cross-section when the G11 global normalization is used (blue) and when the g12 dynamic normalization is used (red) for various bins of beam energy above the `MORB` threshold.

1.5 Normalization Uncertainties

The statistical uncertainties of the normalization correction was minimized by ensuring that the statistical sample of the data and `MC` was sufficient in each bin of z-vertex, momentum, $\theta\sin\phi$ and $\theta\cos\phi$. The maximum statistical uncertainty was 0.01%. The systematic uncertainties of the normalization correction was calculated and shown in Sec. 1.5.1.

1.5.1 Track Efficiency Systematic Uncertainty

To calculate the track-efficiency systematic uncertainty, the calculation was redone as described in Sec. 6.2 of the analysis note. The track-efficiency for the systematic study had a binning scheme of θ, ϕ, Fig. 14, instead of the $\theta\sin\phi$, $\theta\cos\phi$ binning seen in Fig. 31 in the analysis note.

Three-charged track-efficiency values from the initial procedure, described
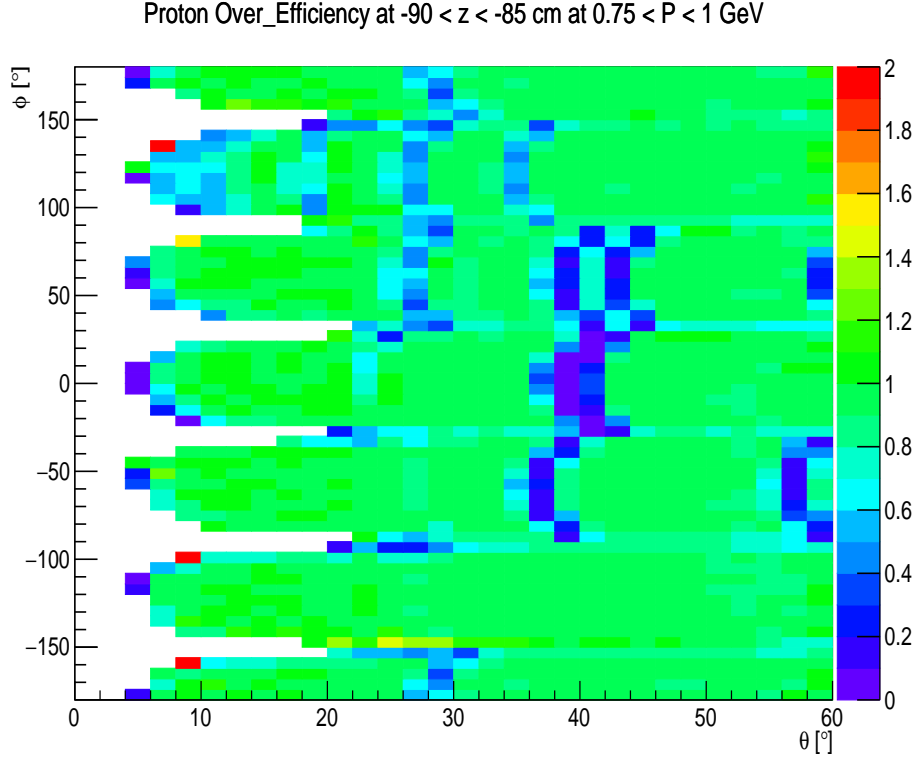
Figure 14: ϕ vs. θ plot showing the over-efficiency of simulating the proton with z-vertex $-90 < z < -85$ cm and momentum $0.75 < p < 1$ GeV from a 2 charged track reaction.

in Sec. 6.2, were compared to the values from this new binning. Since both techniques are not known quantities, the method for calculating the error between the is;

$$\Delta = \frac{x_{previous} - x_{new}}{\frac{x_{previous} + x_{new}}{2}} \qquad (8)$$

where $x_{previous}$ is a value of a three-charged track-efficiency from the mapping of Sec 6.2 and x_{new} is a three-charged track-efficiency from the mapping from the new set of figures derived for this systematic calculation.

Since both values are corrections, it makes little statistical sense to promote one to a "known value", therefore the only appropriate method to measure the error between the values is to use the percent difference method. In this method the denominator is the average value between the two hypotheses, hence the factor of 2.

Angular dependence

To investigate whether there exists a C.M. $\cos\theta$ dependence, the values of Eq. 8 were binned in according with the event C.M. $\cos\theta$, per E_γ value.
  From Figs.[15, 16, 17, 18], there appears that any dependence on $\cos\theta$ is negligible because the relative uncertainty for each $\cos\theta$ value at a certain beam energy is mostly within errors of the neighboring $\cos\theta$ values and the relative shape of the distribution for neighboring $\cos\theta$ values are mostly alike. The only exception for this the 2 bins for $\cos\theta = 0.703$ and $\cos\theta = 0.734$ (Fig. 18), however these 2 bins account for $2/37$ of all $\cos\theta$ bins.
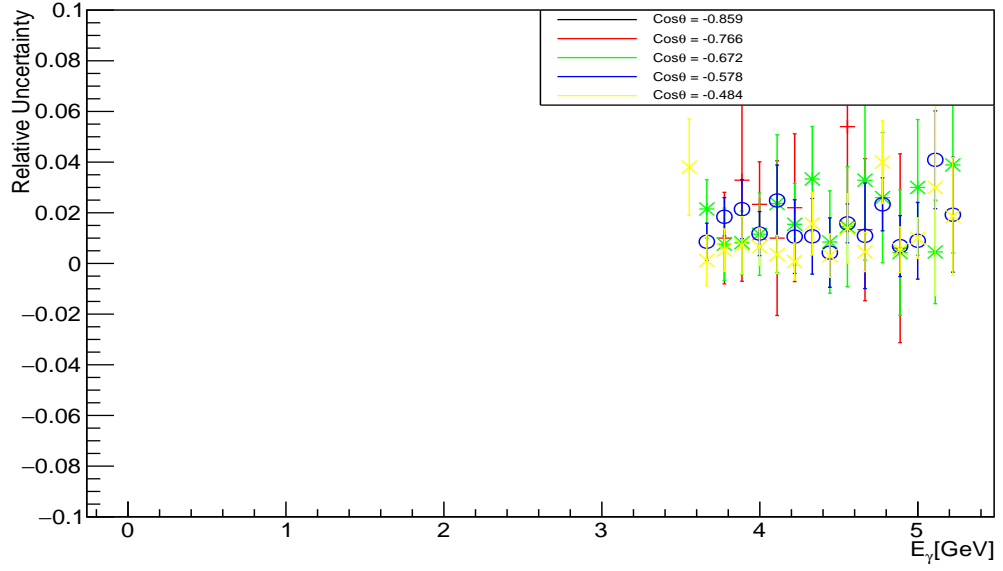
(a) $-0.859 < \cos\theta < -0.484$
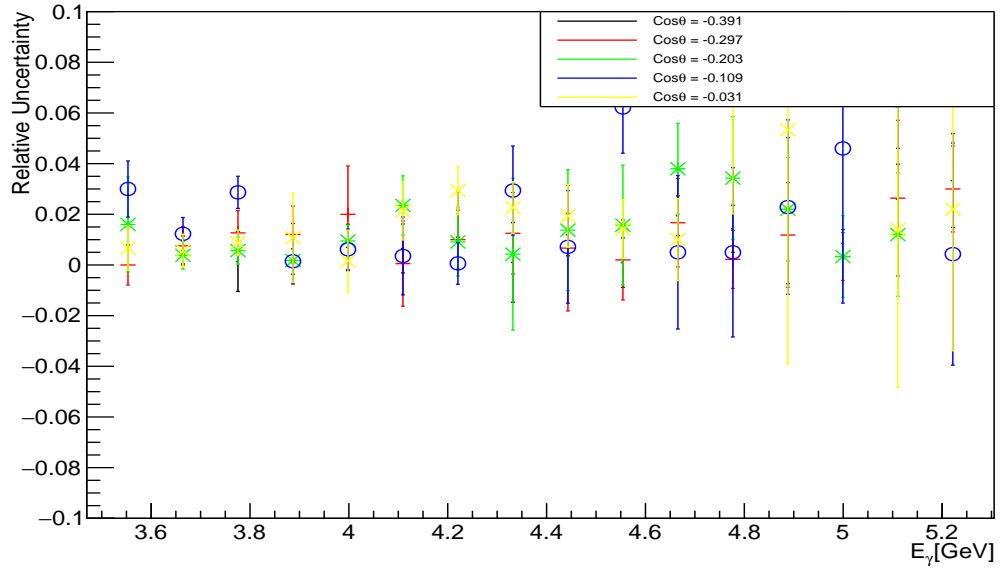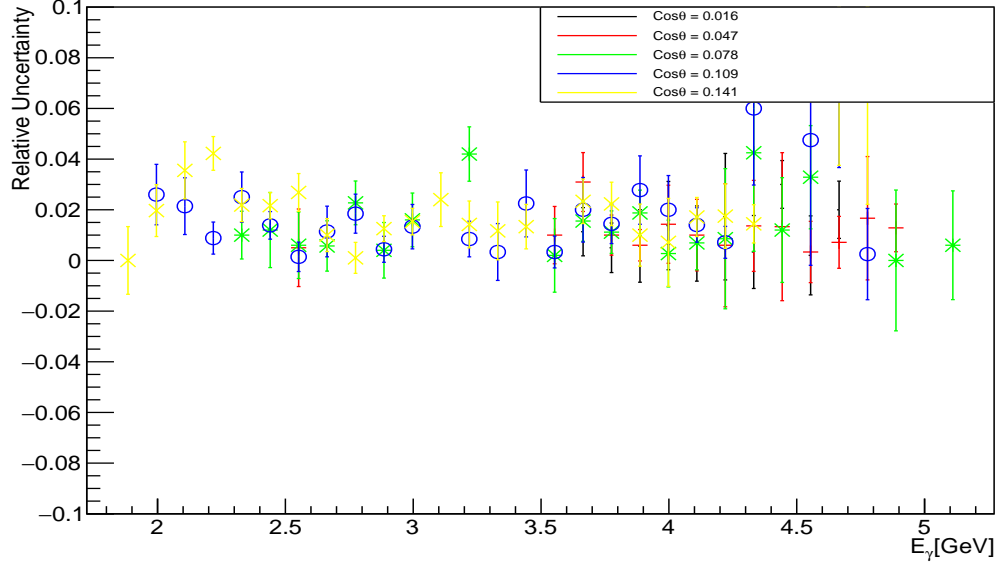

(b) $-0.391 < \cos\theta < -0.031$

Figure 15: (Color Online)Mean relative uncertainty vs. E_γ calculated between the two sets of track efficiencies for $\cos\theta$.

(a) $0.016 < \cos\theta < 0.141$

(b) $0.172 < \cos\theta < 0.297$

Figure 16: (Color Online)Mean relative uncertainty vs. E_γ calculated between the two sets of track efficiencies for $\cos\theta$.

19

(a) $0.328 < \cos\theta < 0.453$

(b) $0.484 < \cos\theta < 0.609$

Figure 17: (Color Online)Mean relative uncertainty vs. E_γ calculated between the two sets of track efficiencies for $\cos\theta$.

20

(a) $0.641 < \cos\theta < 0.766$

21
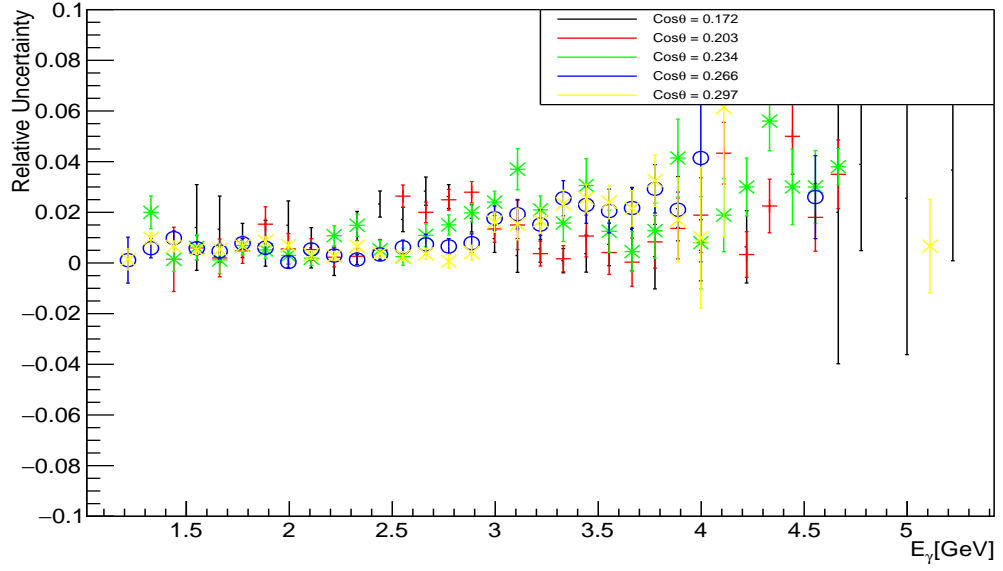(b) $0.797 < \cos\theta < 0.828$

Figure 18: (Color Online)Mean relative uncertainty vs. E_γ calculated between the two sets of track efficiencies for $\cos\theta$.
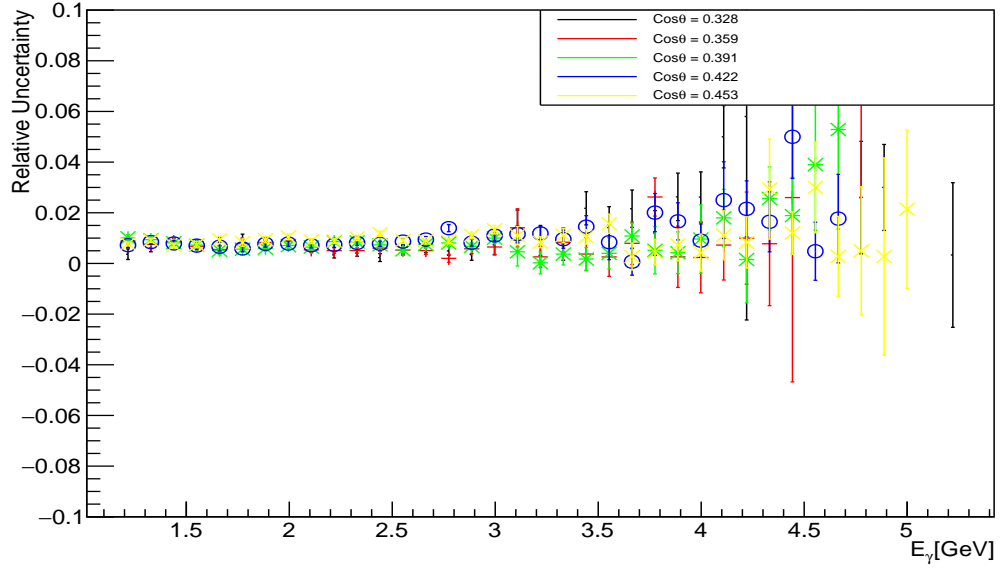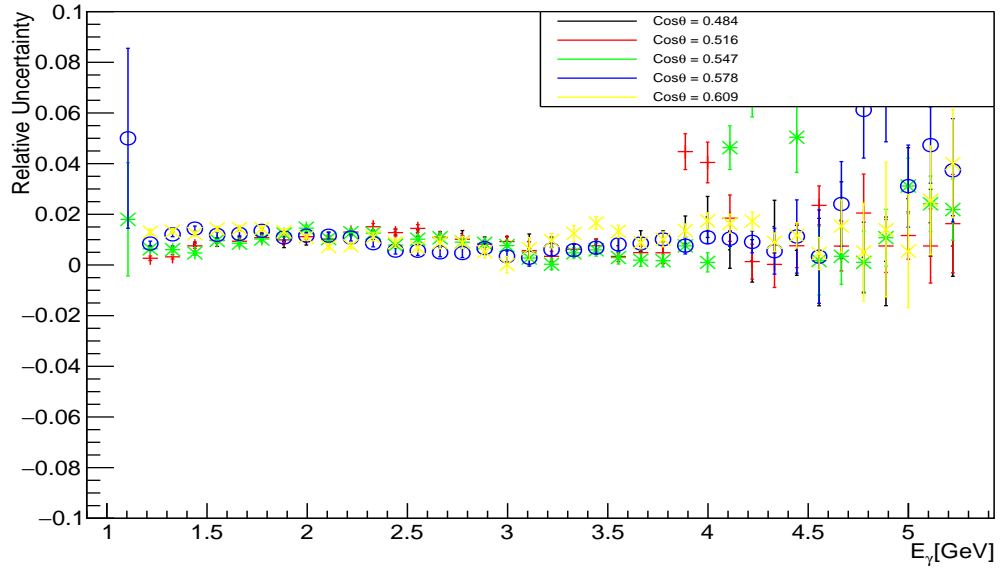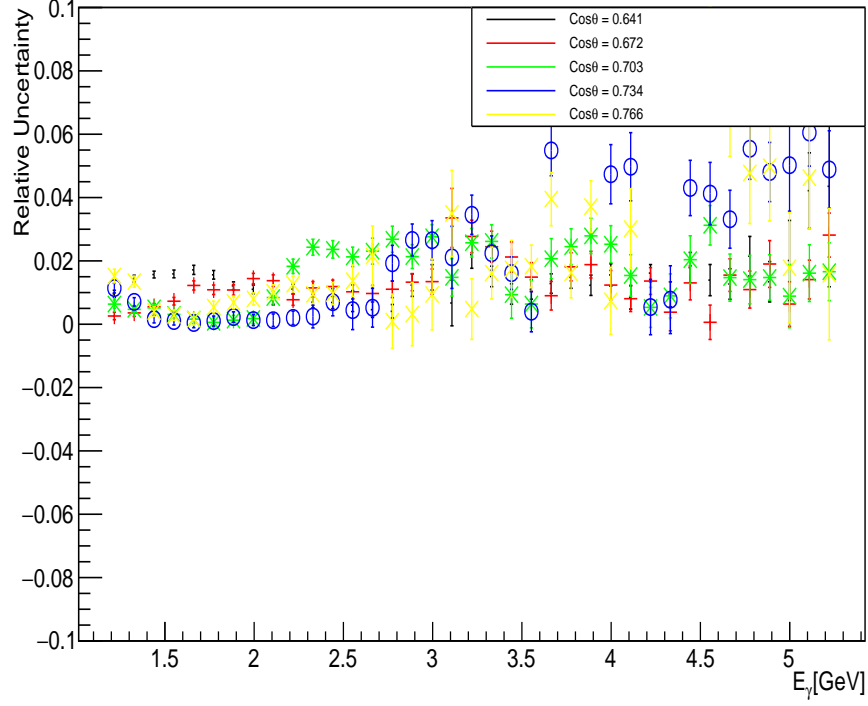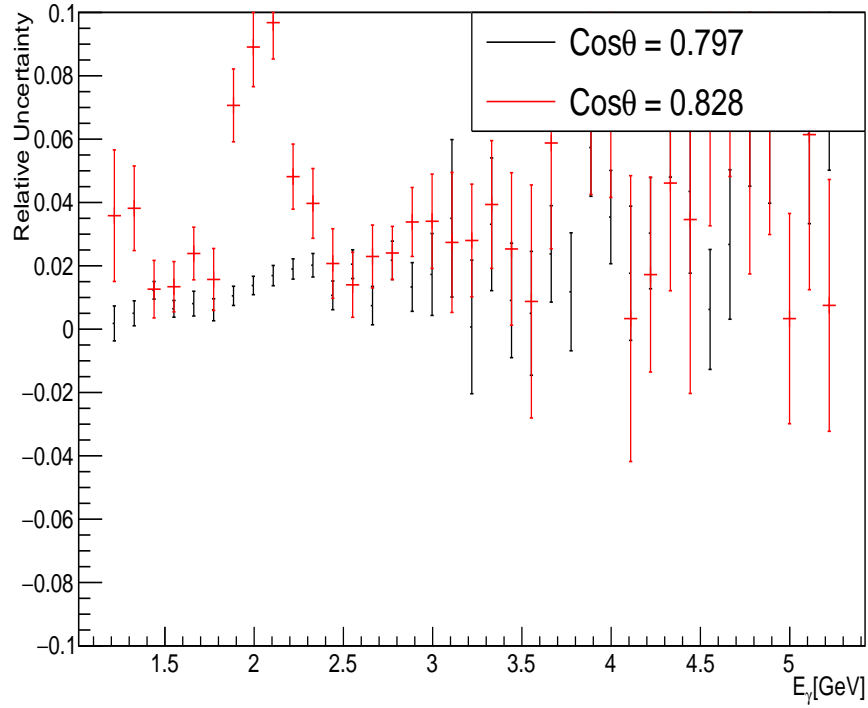
Incident photon (E_γ) dependence

To investigate whether there exists a C.M. $\cos\theta$ dependence, the values of Eq. 8 were binned in according with the event C.M. $\cos\theta$. To investigate whether there exists a dependence to the variable of incident beam energy (E_γ), the values of Eq. 8 were binned in according with the event E_γ. Two regions were chosen, the "Lep Trigger" region, which consists of incident beam energies between 1.1 –3.6 GeV and the "MOR" region, which consists of incident beam energies between 3.6 –5.5 GeV. Figure 19 and Fig. 20 depict the mean value of Eq. 8 for bins of C.M.$\cos\theta$ and incident beam energy for the "Lep Trigger" and "MOR trigger" regions respectively.
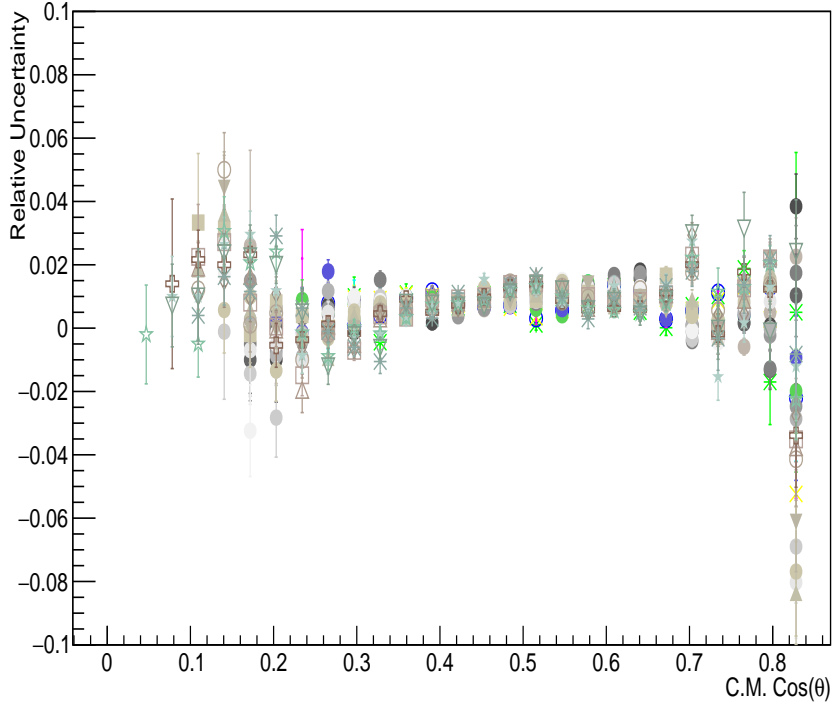
Figure 19: Mean relative uncertainty vs. $\cos\theta$ calculated between the two sets of track efficiencies for incident beam energy between 1.2–3.6 GeV. Multiple points in $\cos\theta$ are bins of incident beam energy.
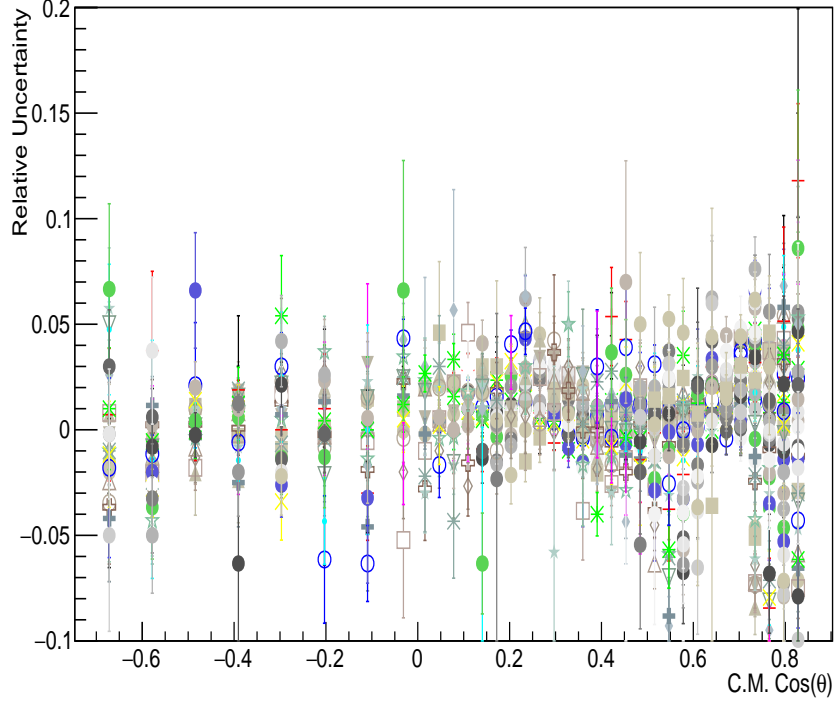
Figure 20: Mean relative uncertainty vs. $\cos\theta$ calculated between the two sets of track efficiencies for incident beam energy between 3.6–5.5 GeV. Multiple points in $\cos\theta$ are bins of incident beam energy.

Therefore, to investigate the dependence on incident beam energy the mean value for all C.M. $\cos\theta$ bins per incident beam energy were plotted, example plots for this can be seen in Fig. 21. The mean and RMS track-efficiency systematic uncertainty value from each incident beam energy was added in quadrature and plotted as a function of incident beam energy. This distribution was then fit to a 2nd order polynomial and the values of the polynomial were taken to be the systematic uncertainty for the track-efficiency, which is dependent on incident beam energy. This fit and distribution can be seen in Fig. 22.

23
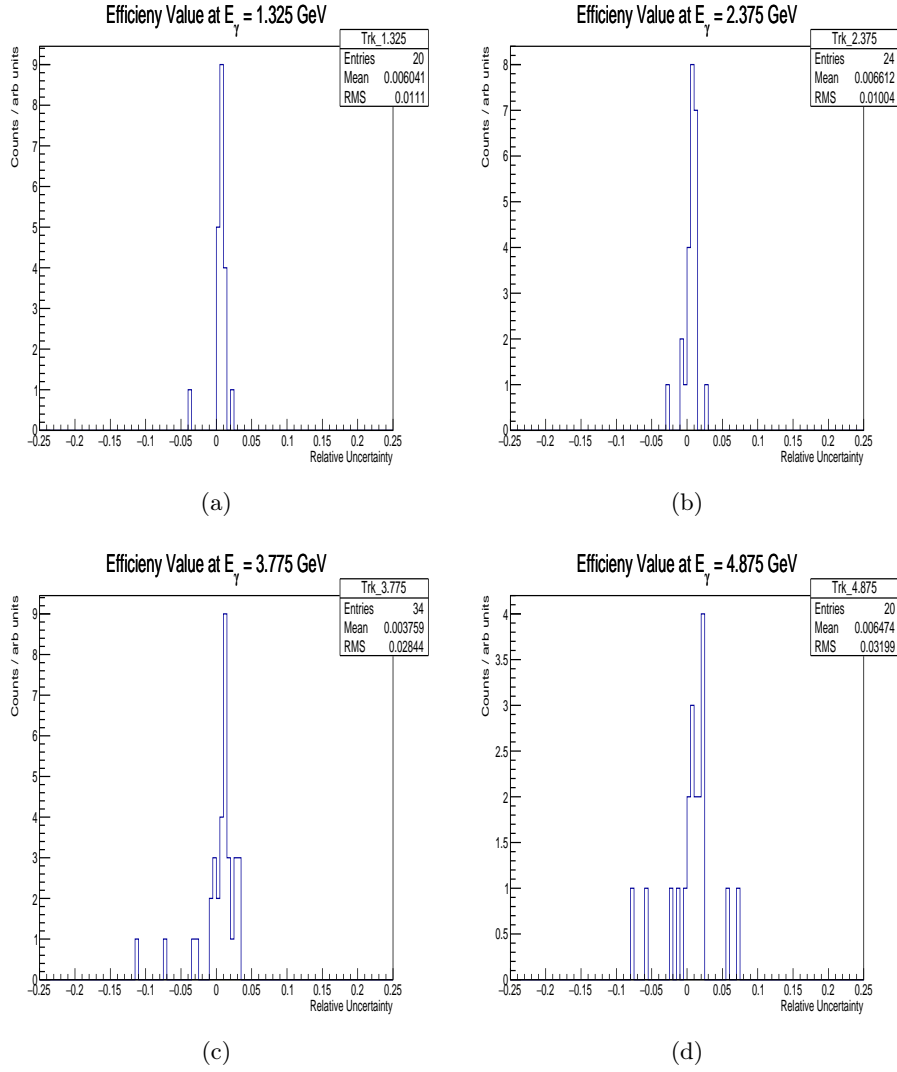
Figure 21: Mean value per incident beam energy 1.325 GeV(a), 2.375 GeV(b), 3.775 GeV(c), 4.875 GeV(d).
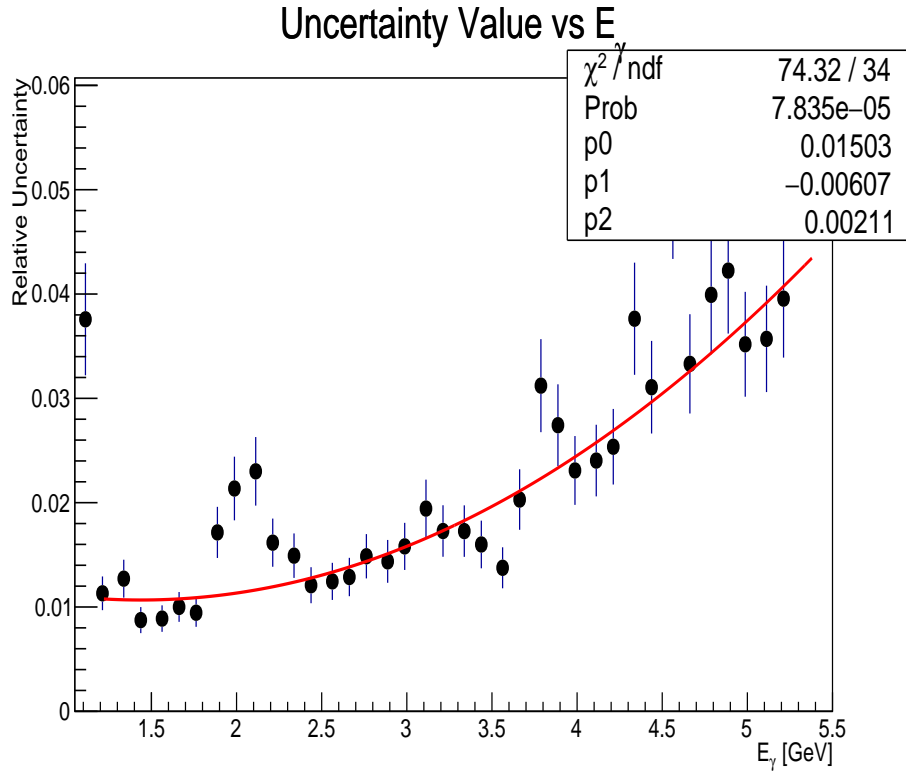
Figure 22: (Color-online)Relative error calculated between the two sets of track efficiencies as a function of incident beam energy (black points). Fit consisting of a 2nd order polynomial to the data (red line).

2 Code Templates

If you are going to use kinematic fitting for this analysis, please use the kinematic fitter codes found on the g12 wiki. If your main analysis does not use kinematic fitting, please do not use it to calculate the track efficiency

`https://clasweb.jlab.org/rungroups/g12/wiki/index.php/G12_Corrections_and_Kinematic_Fitting`

Code templates can be found at `https://github.com/mckunkel/G12_Corrections/tree/master/Efficiency`. The file '*EfficiencyCodes.tar*' is a packed tar file that has code templates for the user to model their study against. Its advisable to read the codes and the following sections before using the codes. To untar the file;

```
tar -xf EfficiencyCodes.tar
```

this will produce a folder
'*EfficiencyCodes*'
which contains the folders

- BOSSkimCodes

- Data

- MC

- MakeEffs

2.1 Data Processing Codes

The folder '*BOSSkimCodes*' contains the folders

- PIM_EFF

- PIP_EFF

- PROT_EFF

and the source file

- buildCentos65.cshrc

with each containing the skim codes to be used on the output of `A1c`. It is important that these executables be used for both data and Monte-Carlo. Most of the skimming procedures start around lines 331 of the Ppp_cE.cc files. These files are responsible for creating a ROOT file with all the needed features for this type of study. To build these scripts, please update the

- buildCentos65.cshrc

file to the CENTOS version on JLab cluster and source the script

```
source buildCentos65.cshrc
```

then in each folder

```
scons Ppp_cE.cc
```

If there are any problems building this software, please contact the `CLAS` librarian and inquire about the build system for the `CLAS6` software.

2.2 Data Processing Pipeline

In the folders

- Data
- MC/SimulationCodes

are submit scripts written in PERL that need to be modified by the user to ensure the proper pipeline. There are helper scripts

- Data/EXECUTABLES/get_codes.bash
- MC/SimulationCodes/get_codes.bash

that help putting the needed executables in their proper place. However, pipelining the procedure is standard CLAS procedure, so this will not be covered in detail here.

2.3 Making Track Efficiency Plots

In the folders

- EfficiencyCodes/MakeEffs/X

,where X is the particle name, are codes to help the user make the maps for both MC and data. The codes starting with name

- Make_*.C

are templates used to create various mappings that were tested. The ones used for analysis were derived from

- Make_X_Efficiency.C

- Make_X_Efficiency_MC.C

where X is the particle name. The other scripts were in beta testing, use responsibly.

The codes that have name similar to

- Compare_*_new.C

create the mapping and ROOT file for lookup. Once all of this is done, create a lookup script similar to below and happy analyzing.

```
TString P_value = Prot_Hist_num(Vz,P_Ptot_fit);

//cout<<P_value<<" "<<Ep_value<<" "<<Em_value<<endl;


if (P_value =="") {
event_prot_eff = 0.0;
//cout<<Vz<<endl;
}
else{
TH2D *hEff_P= (TH2D*)P_Data.Get(P_value);
for (int x = 1; x<=hEff_P->GetNbinsX(); x++) {
for (int y = 1; y<=hEff_P->GetNbinsY(); y++) {
if (abs(P_Theta_fit*sin(P_Phi_fit*TMath::Pi()/180.) -
    hEff_P->GetXaxis()->GetBinCenter(x)) <= 4. &&
    abs(P_Theta_fit*cos(P_Phi_fit*TMath::Pi()/180.) -
    hEff_P->GetYaxis()->GetBinCenter(y)) <= 4.) {
//cout<<hEff_plot->GetBinContent(x,y)<<endl;
event_prot_eff = hEff_P->GetBinContent(x,y);
}
//cout<<hPimEff_I_II->GetBinContent(x,y)<<"
    "<<hEff_plot->GetBinContent(x,y)<<endl;
}
}
}
```

```
TString Prot_Hist_num(Double_t z, Double_t p){


//cout<<"I am active"<<endl;
if (z <= -105. ){

if (p <= 0.5 && p > 0. ) {
return "hProtEff_I_I";
}
```

```
else if (p <= 0.75 && p > 0.5 ) {
return "hProtEff_I_II";
}

else if (p <= 1. && p > 0.75 ) {
return "hProtEff_I_III";
}

else if (p <= 1.5 && p > 1. ) {
return "hProtEff_I_IV";
}

else if (p <= 2. && p > 1.5 ) {
return "hProtEff_I_V";
}

else if (p <= 2.5 && p > 2. ) {
return "hProtEff_I_VI";
}

else if (p <= 3. && p > 2.5 ) {
return "hProtEff_I_VII";
}

else if ( p > 3. ) {
return "hProtEff_I_VIII";
}

else {
cout<<"NOT IN BOUNDS WITH MOMENTUM"<<endl; return "";
}

}

else if (z <= -100. && z > -105. ){

if (p <= 0.5 && p > 0. ) {
return "hProtEff_II_I";
}

else if (p <= 0.75 && p > 0.5 ) {
return "hProtEff_II_II";
}

else if (p <= 1. && p > 0.75 ) {
return "hProtEff_II_III";
}

else if (p <= 1.5 && p > 1. ) {
```

```cpp
return "hProtEff_II_IV";
}

else if (p <= 2. && p > 1.5 ) {
return "hProtEff_II_V";
}

else if (p <= 2.5 && p > 2. ) {
return "hProtEff_II_VI";
}

else if (p <= 3. && p > 2.5 ) {
return "hProtEff_II_VII";
}

else if ( p > 3. ) {
return "hProtEff_II_VIII";
}

else {
cout<<"NOT IN BOUNDS WITH MOMENTUM"<<endl; return "";
}

}

else if (z <= -95. && z > -100. ){

if (p <= 0.5 && p > 0. ) {
return "hProtEff_III_I";
}

else if (p <= 0.75 && p > 0.5 ) {
return "hProtEff_III_II";
}

else if (p <= 1. && p > 0.75 ) {
return "hProtEff_III_III";
}

else if (p <= 1.5 && p > 1. ) {
return "hProtEff_III_IV";
}

else if (p <= 2. && p > 1.5 ) {
return "hProtEff_III_V";
}

else if (p <= 2.5 && p > 2. ) {
return "hProtEff_III_VI";
```

```cpp
        }

        else if (p <= 3. && p > 2.5 ) {
        return "hProtEff_III_VII";
        }

        else if ( p > 3. ) {
        return "hProtEff_III_VIII";
        }

        else {
        cout<<"NOT IN BOUNDS WITH MOMENTUM"<<endl; return "";
        }

    }

    else if (z <= -90. && z > -95. ){

        if (p <= 0.5 && p > 0. ) {
        return "hProtEff_IV_I";
        }

        else if (p <= 0.75 && p > 0.5 ) {
        return "hProtEff_IV_II";
        }

        else if (p <= 1. && p > 0.75 ) {
        return "hProtEff_IV_III";
        }

        else if (p <= 1.5 && p > 1. ) {
        return "hProtEff_IV_IV";
        }

        else if (p <= 2. && p > 1.5 ) {
        return "hProtEff_IV_V";
        }

        else if (p <= 2.5 && p > 2. ) {
        return "hProtEff_IV_VI";
        }

        else if (p <= 3. && p > 2.5 ) {
        return "hProtEff_IV_VII";
        }

        else if ( p > 3. ) {
        return "hProtEff_IV_VIII";
        }
```

```cpp
else {
cout<<"NOT IN BOUNDS WITH MOMENTUM"<<endl; return "";
}


}

else if (z <= -85. && z > -90. ){

if (p <= 0.5 && p > 0. ) {
return "hProtEff_V_I";
}

else if (p <= 0.75 && p > 0.5 ) {
return "hProtEff_V_II";
}

else if (p <= 1. && p > 0.75 ) {
return "hProtEff_V_III";
}

else if (p <= 1.5 && p > 1. ) {
return "hProtEff_V_IV";
}

else if (p <= 2. && p > 1.5 ) {
return "hProtEff_V_V";
}

else if (p <= 2.5 && p > 2. ) {
return "hProtEff_V_VI";
}

else if (p <= 3. && p > 2.5 ) {
return "hProtEff_V_VII";
}

else if ( p > 3. ) {
return "hProtEff_V_VIII";
}

else {
cout<<"NOT IN BOUNDS WITH MOMENTUM"<<endl; return "";
}


}

else if (z <= -80. && z > -85. ){
```

```cpp
if (p <= 0.5 && p > 0. ) {
return "hProtEff_VI_I";
}

else if (p <= 0.75 && p > 0.5 ) {
return "hProtEff_VI_II";
}

else if (p <= 1. && p > 0.75 ) {
return "hProtEff_VI_III";
}

else if (p <= 1.5 && p > 1. ) {
return "hProtEff_VI_IV";
}

else if (p <= 2. && p > 1.5 ) {
return "hProtEff_VI_V";
}

else if (p <= 2.5 && p > 2. ) {
return "hProtEff_VI_VI";
}

else if (p <= 3. && p > 2.5 ) {
return "hProtEff_VI_VII";
}

else if ( p > 3. ) {
return "hProtEff_VI_VIII";
}

else {
cout<<"NOT IN BOUNDS WITH MOMENTUM"<<endl; return "";
}

}

else if (z <= -75. && z > -80. ){

if (p <= 0.5 && p > 0. ) {
return "hProtEff_VII_I";
}

else if (p <= 0.75 && p > 0.5 ) {
return "hProtEff_VII_II";
}

else if (p <= 1. && p > 0.75 ) {
```

```cpp
    return "hProtEff_VII_III";
    }

    else if (p <= 1.5 && p > 1. ) {
    return "hProtEff_VII_IV";
    }

    else if (p <= 2. && p > 1.5 ) {
    return "hProtEff_VII_V";
    }

    else if (p <= 2.5 && p > 2. ) {
    return "hProtEff_VII_VI";
    }

    else if (p <= 3. && p > 2.5 ) {
    return "hProtEff_VII_VII";
    }

    else if ( p > 3. ) {
    return "hProtEff_VII_VIII";
    }

    else {
    cout<<"NOT IN BOUNDS WITH MOMENTUM"<<endl; return "";
    }

    }

    else if (z > -75. ){

    if (p <= 0.5 && p > 0. ) {
    return "hProtEff_VIII_I";
    }

    else if (p <= 0.75 && p > 0.5 ) {
    return "hProtEff_VIII_II";
    }

    else if (p <= 1. && p > 0.75 ) {
    return "hProtEff_VIII_III";
    }

    else if (p <= 1.5 && p > 1. ) {
    return "hProtEff_VIII_IV";
    }

    else if (p <= 2. && p > 1.5 ) {
    return "hProtEff_VIII_V";
```

```cpp
}

else if (p <= 2.5 && p > 2. ) {
return "hProtEff_VIII_VI";
}

else if (p <= 3. && p > 2.5 ) {
return "hProtEff_VIII_VII";
}

else if ( p > 3. ) {
return "hProtEff_VIII_VIII";
}

else {
cout<<"NOT IN BOUNDS WITH MOMENTUM"<<endl; return "";
}

}

else {
//cout<<"NOT IN BOUNDS WITH z VERTEX"<<endl;
return "";
}

//cout<<"I am at the end "<<z<<" "<<p<<endl;

}
```

Compare

References

[1] G12 Experimental Group. g12 Analysis Procedures, Statistics and Systematics. Technical report, CLAS-NOTE 2017 - 002, 2017.

[2] M. C. Kunkel et al. Exclusive photoproduction of π^0 up to large values of mandelstam variables s, t, and u with CLAS. *Phys. Rev. C*, 98:015207, Jul 2018.